IOPscience iopscience.iop.org

Home Search Collections Journals About Contact us My IOPscience

Elastic properties of single-crystalline and consolidated nano-structured yttrium oxide at room temperature

This article has been downloaded from IOPscience. Please scroll down to see the full text article.

2000 J. Phys.: Condens. Matter 12 5403

(http://iopscience.iop.org/0953-8984/12/25/305)

View the table of contents for this issue, or go to the journal homepage for more

Download details:
IP Address: 171.66.16.221
The article was downloaded on 16/05/2010 at 05:15

Please note that terms and conditions apply.

J. Phys.: Condens. Matter **12** (2000) 5403–5409. Printed in the UK PII: S0953-8984(00)10550-8

Elastic properties of single-crystalline and consolidated nano-structured yttrium oxide at room temperature

J Baller†, J K Krüger†, R Birringer‡ and C Proust§

† Universität des Saarlandes, Experimentalphysik 10.2, Bau 38, Postfach 151150 D-66041, Saarbrücken, Germany

‡ Universität des Saarlandes, Technische Physik 10.3, Bau 43B, Postfach 151150 D-66041, Saarbrücken, Germany

§ CRPHT–CNRS, 45071 Orléans Cédex 2, France

Received 23 December 1999

Abstract. High resolution Brillouin spectroscopy was used to characterize the elastic stiffness properties of consolidated nano-crystalline yttrium oxide as well as of the related single-crystalline state. Defect enriched grain boundaries are discussed as sources for the extremely soft elastic properties of the nano-crystalline state.

1. Introduction

The influence of the particle size of nano-structured materials on their acoustic properties is still a matter of debate [1–3]. Less attention has been paid to the influence of the mesoscopic morphology appearing in the consolidated nano-structured bulk samples on the mechanical and optical properties. In this work we present the complete elastic data for single crystalline cubic yttrium oxide (sc-Y_2O_3) at room temperature. These data are compared to those obtained from nano-structured consolidated samples (nc-Y_2O_3). Whereas the elastic light scattering is strongly affected by the mesoscopic morphology, the acoustic properties are dominated by the nano-structure.

2. Experiment

2.1. Samples and sample preparation

At room temperature sc-Y_2O_3 has body-centred cubic symmetry with space group $Ia3$ (T_h^7). The mass density is 5033 kg m^{-3} and the refraction index is 1.9435 at 514.4 nm [4].

The sc-Y_2O_3 sample under study consists of a small platelike fragment of $4 \times 4 \times 0.2$ mm^2. It was grown by the flame fusion method (Verneuil process) [12]. X-ray diffraction patterns were recorded for three different locations on the sample surface. All three measurements led to the same Miller indices (320) for the surface plane.

Our nano-crystalline Y_2O_3 (nc-Y_2O_3) was made by noble gas condensation and subsequent consolidation in vacuum at 1.5 GPa [5]. It has the same cubic symmetry as our sc-Y_2O_3. The sample under study has a platelike shape and a thickness of about 12 μm. It is opaque and shows very strong elastic scattering at optical wavelengths. Due to the cubic symmetry of the nano-particles and due to the crystallite size of about 17 nm, this elastic scattering was not expected. Obviously, the consolidation process caused optical heterogeneities on a mesoscopic length scale resulting in Mie scattering.

0953-8984/00/255403+07$30.00 © 2000 IOP Publishing Ltd

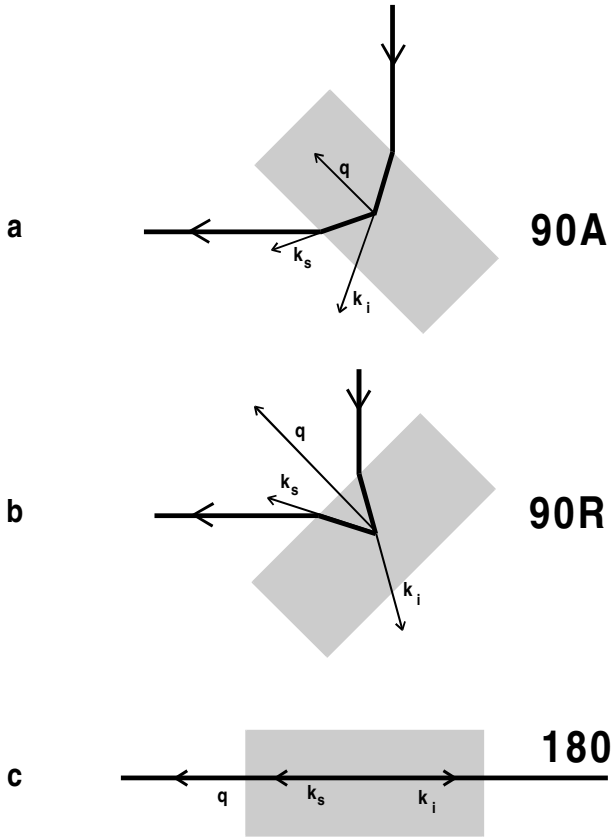

Figure 1. 90A, 90R and 180 scattering geometries. $\boldsymbol{k}_i$, $\boldsymbol{k}_s$: wavevectors of the incident laser beam and of the scattered light, respectively. $\boldsymbol{q}$: phonon wavevector.

2.2. Brillouin spectroscopy

Our Brillouin measurements were performed using a six-pass Tandem Fabry–Pérot interferometer described elsewhere [6]. Figure 1 schematically shows the 90A, 90R and 180 scattering geometries used in this work.

In order to protect the photo-multiplier from the strong elastically scattered light, we introduced a fast switching mechanical shutter in front of the detector. The optical signal needed to stabilize the spectrometer is fed to a second, less sensitive photo-multiplier.

3. Results and discussion

90A Brillouin scattering (figure 1(a)) has been used to determine the elastic properties of sc-Y_2O_3. According to [6] and [7], the 90A-scattering technique confines the phonon wavevector within the sample plane (320). Then, the relation between the sound velocity v, the vacuum laser wavelength λ_0 (= 514.5 nm), the phonon frequency f^{90A} and the phonon wave length λ^{90A}, is given by [6, 7]:

$$v^{90A} = f^{90A}\Lambda^{90A} \simeq \frac{\lambda_0 f^{90A}}{\sqrt{2}}.$$

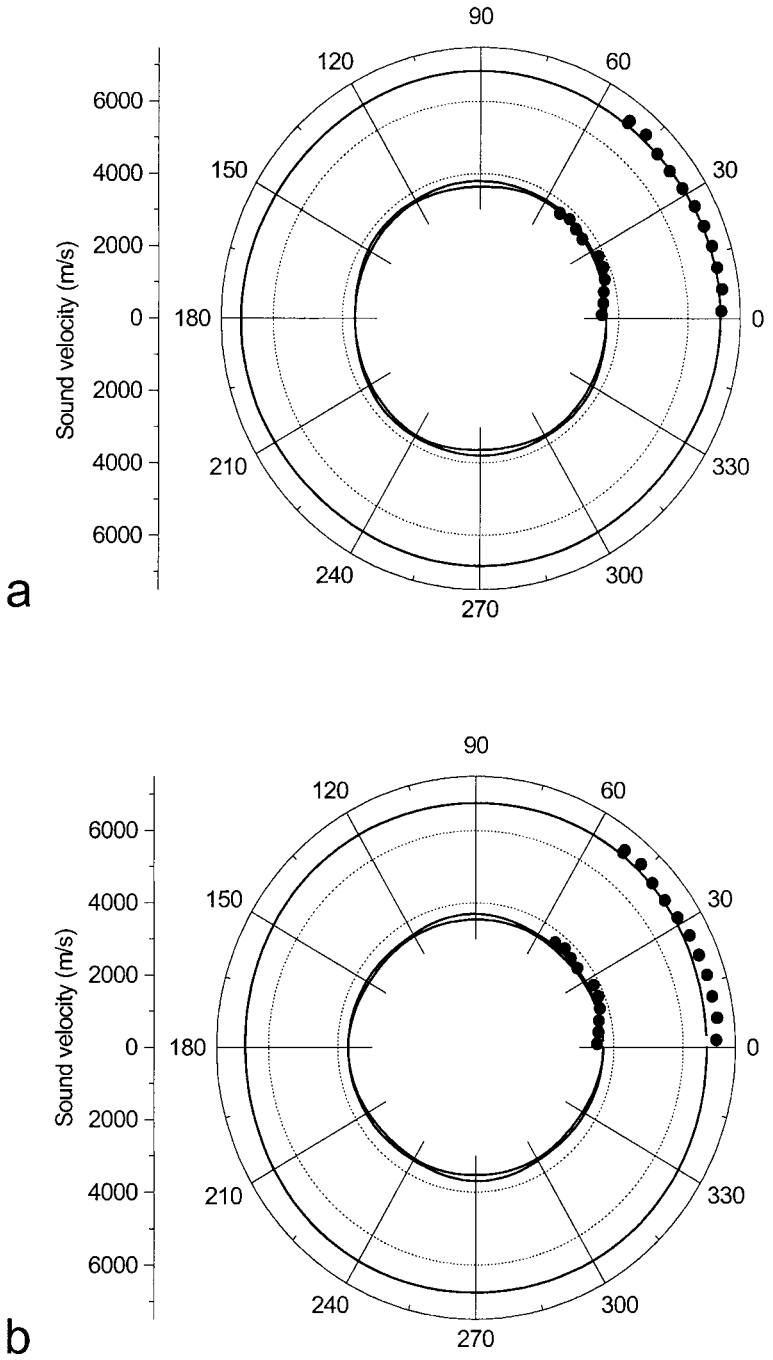

Figure 2. Polar plots of measured sound velocities and graphs of corresponding fit functions for the (320) plane. (a) Fit done with c_{11}, c_{12} and c_{44} as parameters. (b) Fit done with fixed c_{11} according to [8] and c_{12} and c_{44} as parameters.

By turning the sample around an axis perpendicular to the sample plane, we measured the quasi-longitudinal and quasi-transversal sound velocities within the plane (figure 2(a)).

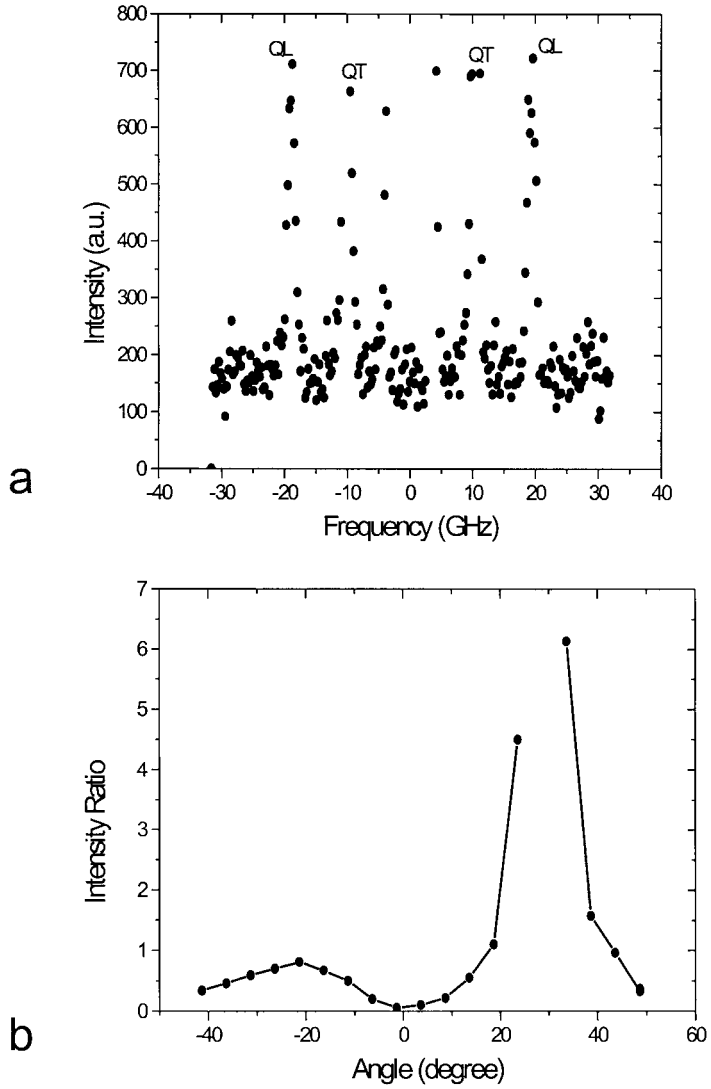

Figure 3. Brillouin measurements of sc-Y_2O_3. (a) Spectrum recorded in the 90A scattering geometry. QL: quasi-longitudinal phonon line. QT: quasi-transversal phonon line. (b) Intensity of the quasi-longitudinal phonon line divided by the intensity of the quasi-transversal phonon line as a function of the turning angle in the (320) plane.

During the measurements, a significant exchange of intensities between the quasi-longitudinal polarized phonon (QL) and the quasi-transversal polarized phonon (QT) dependent on the turning angle could be observed (figure 3). This effect can be put down to an angle dependency of the opto-acoustic coupling. The corresponding attenuation data show no significant variation.

Figure 2(a) shows the polar plot of the measured sound velocities and the graphs of the corresponding fit functions for the (320) plane. The fit results yield the complete elastic tensor [8]:

$c_{11} = 240.35 \pm 0.02$ GPa $\quad c_{12} = 99.40 \pm 0.02$ GPa $\quad c_{44} = 65.69 \pm 0.01$ GPa.

(Error values result from the fit procedure.)

Since the elastic stiffness coefficients of sc and microstructured (mc) samples should only differ by an orientation average [9, 10], we compare our results to measurements of elastic properties made by Desmaison-Brut *et al* [11].

Our value of c_{11} is in good agreement with $c_{11} = 239.65$ presented in [11] for a consolidated sample of microstructured Y_2O_3 (particle size 1–10 μm).

In a previous paper [12], one of the authors (CP) investigated the same crystal and measured the elastic constant $c_{11} = 244$ GPa and the linear combination $(c_{11} + c_{12})/2 + c_{44} = 247$ GPa at room temperature.

In this work, measurements were improved using a high resolution more accurate spectrometer and the three constants could be determined. The present values for c_{11} and the linear combination differ respectively by about 7 and 5% from those given by Proust *et al* [12]. In figure 2(b), we held c_{11} fixed at the value given in [12] and tried to fit our data by varying c_{12} and c_{44}. Obviously the fixed c_{11} value is too small to fit our data. The resulting chi-square is twice as big as the value obtained by fitting with three parameters. Since we used in this work a piece of the same host crystal as used in the previous study, the reason of the discrepancy observed is not clear: it may be partly related to the optical quality of the crystal: the crystal was synthesized by the Verneuil method. It is very difficult to obtain single crystals of good optical quality because the powder is fused at high temperature (melting point 2680 K) and during cooling the crystal is subject to important internal stress. Moreover, a phase transition occurs from the high-temperature hexagonal form to the cubic form and induces defects such as cleavage planes corresponding to the (111) planes of the cubic crystal.

The nano-crystalline sample was investigated using 90A and 180 scattering geometries. The related Brillouin spectra are given in figure 4. These spectra remarkably differ from those of the single crystal (figure 3). The 90A spectrum of nc-Y_2O_3 (figure 4(a)) shows two rather sharp phonon lines located on a broad intensity shoulder. The gaps in the centre and at both sides of the spectrum are caused by the shutter. The velocity of the longitudinal sound mode could be determined to be $v = 3350$ m s^{-1}.

A remarkable fact from the 90A measurement is the end of the intensity shoulder at about 25 GHz (see figure 4(a)). It is only visible at the right side of the spectrum because of a slightly asymmetric behaviour of the shutter, which hides this edge at the left side. The position of the edge roughly coincides with the position of the phonon lines, measured in back-scattering (figure 4(b)). We explain the spectral feature of the 90A scattering as follows.

As a consequence of the massive optical and acoustical heterogeneity on meso- and macroscopical scales, we state the occurrence of multiple light refraction within the sample which is caused by Mie scattering. This means that the incident light wave not only propagates along k_i^{90A} but also is scattered to all other directions. The wavevector of the k_i^{180} scattering geometry leads to a maximum value of the scattering vector $\boldsymbol{q}$ (figure 1) which in turn leads to an upper bound for the hypersonic sound frequency and is therefore a limit for the spectral intensity distribution. The appearance of the two rather sharp phonon lines in figure 4 is attributed to the radiation pattern of the Mie scattering [13] which shows highest intensity along the optical scattering vectors.

It should be remembered that a perfectly consolidated nc-material consisting of cubic nc-crystals of 17 nm diameter should be rather transparent. The optical behaviour should be described by only one refractive index which should coincide with that of the single crystal.

Indeed, the refractive index of nc-Y_2O_3 deduced from the 180 and 90A measurements $n = f^{180}/f^{90A}\sqrt{2} \approx 1.92$ [6], is almost identical to the refractive index of the single crystal. This implies that the observed mesoscopic optical heterogeneity only slightly affects the average refractive index compared to the single crystal indicating the presence of only a

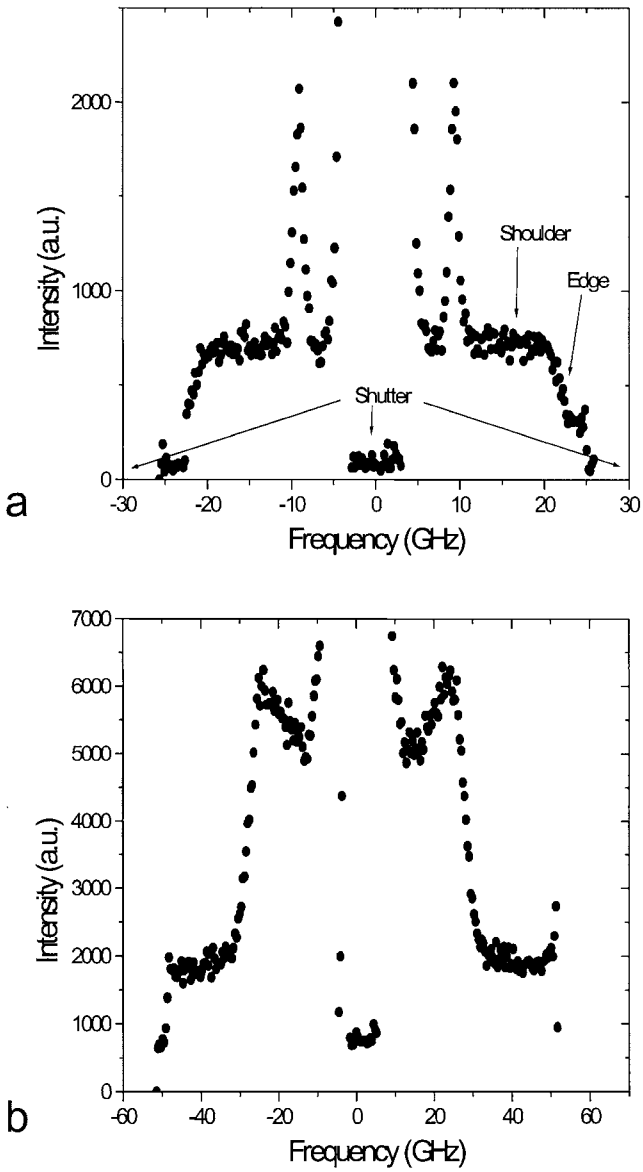

Figure 4. Brillouin measurements of nc-Y_2O_3. (a) Spectrum recorded in the 90A scattering geometry. (b) Spectrum recorded in the 180 scattering geometry.

limited amount of optical very efficient defects (voids) per volume. Taking into account that the refraction index does almost not change between the sc- and the nc-state it seems reasonable to assume that the same holds true for the specific refractivity. Provided that the Lorentz–Lorenz relation can be applied it then turns out that our nc-sample has almost the mass density of the sc-state. On that background the rather high optical scattering efficiency of the nc-sample has its origin in surface defects rather than in volume defects. Therefore, we believe that the defects are concentrated in inner surfaces (two-dimensional voids) of mesoscopic size located between well consolidated grain clusters.

With the relation $c_{11} = \rho v^2$ [6], with ρ being the density of the nano-crystalline material, the elastic stiffness coefficient c_{11} of the nc-sample can be calculated. Since the mass density of the nano-crystalline material was not known, we used the single-crystalline density of 5033 kg m^{-3} as an upper limit for the density of the nano-crystalline state. The resulting stiffness coefficient amounts to 56 GPa. Compared to the sc and mc [11] stiffness coefficient, this signifies a reduction by a factor of four.

In [14] Krüger *et al* showed that for Ca-modified lead titanate (PCT) c_{11} of nc-samples of PCT can be higher as well as lower than c_{11} of mc-samples depending on the grain size of the nc-material, but both values maximally differ by a factor of 0.7. For nc- and mc-diamond, the difference of the elastic stiffness coefficients is even smaller [10]. The nc- and mc-samples of PCT investigated by Krüger *et al* [14] were produced by successive annealing of pure amorphous material whereas the diamond samples [10] were produced by chemical vapour deposition.

This leads to the conclusion that the additional consolidation process of the nc-Y_2O_3 sample is responsible for the above mentioned inner surfaces which strongly dominate the macroscopic elastic behaviour and therefore lead to the significant softening of c_{11} of the consolidated sample. This hypothesis is supported by the above mentioned unexpected appearance of strong Mie scattering of the nc-Y_2O_3 sample due to two-dimensional voids which have no equivalence in the perfectly consolidated samples [10, 14]. This result shows that if one wants to compare the physical properties of nc- and sc-samples, the influence of structures caused by the preparation process of nc-samples can lead to wrong conclusions about their physical properties.

Acknowledgment

This work was kindly supported by the *Sonderforschungsbereich* 277.

References

[1] Gleiter H 1989 *Prog. Mater. Sci.* **33** 223
[2] Gleiter H 1992 *Nanostruct. Mater.* **1** 1
[3] Gleiter H 1995 *Nanostruct. Mater.* **6** 3
[4] Tropf W J and Thomas M E 1991 *Handbook of Optical Constants of Solids II* p 1079
[5] Birringer R, Gleiter H, Klein H-P and Marquardt P 1984 *Phys. Lett.* A **102** 365
[6] Krüger J K 1989 *Optical Techniques to Characterize Polymer Systems* ed H Bässler (Amsterdam: Elsevier)
[7] Krüger J K, Marx A, Peetz L, Roberts R and Unruh H-G 1986 *Colloid. Polym. Sci.* **264** 403
[8] Auld B A 1973 *Acoustic Fields and Waves in Solids* (New York: Wiley)
[9] Krüger J K, Embs J P, Lukas S, Hartmann U, Brierley C J, Beck C M, Jiménez R, Alnot P and Durand O 2000 *J. Appl. Phys.* **87** 74
[10] Krüger J K, Embs J P, Lukas S, Hartmann U, Brierley C J, Beck C M, Jimenez R and Alnot P 2000 *Diamond Relat. Mater.* **9** 123
[11] Desmaison-Brut M, Montintin J, Valin E and Boncoeur M 1995 *J. Am. Ceram. Soc.* **78** 716
[12] Proust C, Vaills Y, Luspin Y and Husson E 1995 *Solid State Commun.* **39** 729
[13] Born M 1985 *Optik* (Berlin: Springer)
[14] Krüger J K, Ziebert C, Schmitt H, Jiménez B and Bruch C 1997 *Phys. Rev. Lett.* **78** 2240